Hindawi Publishing Corporation
Journal of Spectroscopy
Volume 2016, Article ID 7489536, 11 pages
http://dx.doi.org/10.1155/2016/7489536

Research Article

Ultra-Thin Films of Poly(acrylic acid)/Silver Nanocomposite Coatings for Antimicrobial Applications

Alaa Fahmy,[1] Wael H. Eisa,[2] Mohamed Yosef,[1] and Ali Hassan[1]

[1]*Chemistry Department, Faculty of Science, Al Azhar University, Cairo 11884, Egypt*
[2]*Spectroscopy Department, Physics Division, National Research Center (NRC), Dokki, Cairo 12311, Egypt*

Correspondence should be addressed to Alaa Fahmy; alaa.fahmy@azhar.edu.eg

Received 10 January 2016; Revised 22 March 2016; Accepted 12 April 2016

Academic Editor: Jisheng Pan

In this work not only colloids of poly(acrylic acid) (PAA) embedded with silver nanoparticles (Ag-NPs) but thin films (10 nm) also were deposited using electrospray deposition technique (ESD). A mixture of sodium borohydride ($NaBH_4$) and ascorbic acid (AA) were utilized to reduce the silver ions to generate Ag-NPs in the PAA matrix. Moreover, sodium tricitrate was used to stabilize the prepared colloids. The obtained colloids and films were characterized using UV-visible, transmission electron microscopy (TEM). UV-Vis results reveal that an absorption peak at 425 nm was observed in presence of PAA-$AgNO_3$-AA-citrate-$NaBH_4$. This peak is attributed to the well-known surface plasmon resonance of the silver bound in Ag-NPs, while the reduction was rendering and/or inhibiting in absence of the AA and citrate. FTIR spectroscopy was used to study the mechanism of the reaction process of silver nitrate with PAA. TEM images showed the well dispersion of Ag-NPs in the PAA matrix with average particle size of 8 nm. The antimicrobial studies showed that the Ag-NPs embedded in the PAA matrix have proven to have a significant antimicrobial activity against *E. coli*, *B. subtilis*, and *C. albicans*.

1. Introduction

Surface contamination by pathogenic bacteria, viruses, and fungi is a problem that acquired community contribution to solve it. The most common and important use of antimicrobial coatings has been found in the healthcare setting for sterilization of medical devices [1, 2]. Thus, surface modification of the medical devices obviously reduces the incidence of infections. Strategies that confine antibacterial and/or antifouling property to the surface of the implant, by modifying the surface chemistry and morphology or by encapsulating the material in an antibiotic-loaded coating, are most promising way. Among them, plasma-assisted modifications stand out for their ability to modify various substrates.

As well known, silver metal has a broad and strong antibacterial activity [3]. Firstly, Ag^+ is embedded into polymer matrix by self-assembly of silver ions with polymer template in solution. Subsequently, in situ reduction of silver ions produces polymer/Ag-NPs composites [4]. This method can be used to prepare Ag-NPs which are uniform in shape and size, are convenient in use, and have a pronounced antibacterial effect. Polymers play an important role in the metal-polymer nanocomposites acting as reducing and/or capping agent and, thus, prevent particle growth leading to the aggregation form [5].

Ag-NPs have inspired researchers due to the unique electronic and chemical properties [6]. The interesting color of Ag-NPs gradient in visible spectrum is observed and depending on plasmon resonance. The wavelength of plasmon resonance is correlated to the shape and size of the nanoparticles [7]. Ag-NPs have been showed potential applications in various field of drug delivery [8], water treatment [9], biological science [10], and antibacterial candidates against both Gram (−) and Gram (+) bacteria [11]. Low doses of Ag-NPs are not harmful to human cells thus having broad-spectrum of antibacterial activities. Low concentrations of Ag-NPs inhibit the growth of bacteria with no side effects as compared with traditional antibiotics [12]. The fabrication of silver nanoparticle-containing films and their application as antibacterial materials are widely studied. Nevertheless, this subject is still important.

Polymers embedded with Ag-NPs are well-known antimicrobial agents by virtue of their ability to release the biocidal species, namely, Ag^+ ions in an aqueous environment. The silver cation Ag^+ plays an important role for the antimicrobial activity of silver, which binds strongly to electron donor groups in biological molecules. However, the oxidation of the metallic silver to the active species Ag^+ is possible through an interaction of the silver with the water molecules [13]. Different synthesis methods have been reported for the preparation of Ag-NPs with different sizes, shapes, and size distribution control. The geometric shapes of silver that have been prepared are spherical, tetrahedral, octahedral, cubic, hexagonal, fibers (wires), triangular prisms, disks, and shell, among others [14–17]. Overall, there are somewhat few methods that allow one to systematically make such structures in high yield with control of their architectural parameters. There are series of chemical reductants that have been used for the preparation of noble metal nanoparticles which include sodium borohydride [18, 19], hydrogen gas [20], hydrazine [21], alcohol [22], N,N-dimethylformamide [23], glucose [24], ascorbic acid [25], and heparin [26]; the reduction ability of a reductant plays an important role in the preparation of metal nanoparticles by the reduction reaction. The reducing agents act as electron donor to metal ions which reduced to metal atoms and tend to aggregate because of their high activity; therefore, it is necessary to use stabilizing agents. Kim et al. [27] have reported a facile in situ method for the preparation of poly(acrylic acid) silver nanocomposite with highly dispersed silver nanoparticles. They choose the chemical method to generate silver nanoparticles with a poly(acrylic acid) matrix. The reducing reagent was the primary diamine, polyoxypropylenediamine, which reduced the silver ions. Their data indicated that while silver nanoparticles formed during thermal treatment at 130°C or 160°C were spherical and crystalline, silver nanoparticles formed at 100°C were amorphous. TEM data also showed uniform size distributions for silver nanoparticles with a diameter of around 10 nm.

In this study, poly(acrylic acid)/silver nanocomposite successfully will be prepared through a novel synthetic route by utilizing chemical reduction method; sodium borohydride is used as a strong reducing agent in presence of sodium tricitrate as a surfactant. This pathway will be achieved through simple steps, inexpensive precursors. The prepared Ag nanoparticles are proved to have narrow particle size distribution and a uniform shape. The formation of Ag-NPs will be investigated by UV-Visible spectroscopy and transmission electron microscopy. Fourier transformer infrared spectroscopy (FTIR) is one of the most powerful techniques to investigate a multicomponent system, such as polymer composite. FTIR provides information for both composition and metal-polymer interactions which induces structural changes in the inorganic component and/or polymeric one. These spectral changes combined with other analytical tools may provide a fundamental understanding of inorganic-polymer interaction mechanisms. Furthermore, FTIR spectroscopy used to study the intermolecular interactions exists in the composite. Also it can be used to study the interactions which take place during the formation of polymer complexes [28], miscible blends [29], or aggregates between nanoparticles and polymers [30]. In this work, the interactions between the PAA and the silver nitrate were studied by ATR-FTIR. Morphology of subsequent prepared films by electrospray deposition technique (ESD) will be studied by AFM. According to our knowledge this comparison between the colloid and its ultra-thin films in dependence on structure and activity against pathogenic microorganisms is new and not established until now. Antibacterial activity of the prepared colloid and its films will be tested against Gram negative, Gram positive bacteria, and fungi. The prepared nanocomposite films might potentially be used for surface modifications of medical devices.

2. Experimental

2.1. Materials. Poly(acrylic acid) (M. wt. = 1800 g/mol) and ascorbic acid (99%) were purchased from Sigma-Aldrich Co., USA. Silver nitrate was obtained from Cambrian Chemicals (assay 99%). Trisodium citrate dihydrate ($Na_3C_6H_5O_7 \cdot 2H_2O$ min. assay 99.5%) was received from ADWIC Co. Sodium borohydride (99%) was purchased from Merck, Germany.

2.2. Preparation of PAA/Ag Nanocomposites. Different amounts (0.01, 0.05, 0.1, 0.2, and 0.3) mg of PAA were in each 100 mL methanol with the aid of magnetic stirrer. Thereafter, 0.5 mL of $AgNO_3$ (0.005 M in MeOH) and 1 mL of sodium tricitrate (0.01 M) were added to the selected PAA solution. 10 μL of AA (0.07 M) was added to the above mixture. Finally, 10 μL of ice-cold solution of $NaBH_4$ (0.008 M) was quickly injected to the metal-polymer solution.

2.3. Electrospraying Deposition Technique (ESD). The solutions of the polymer nanocomposite were sprayed through a positively charged metal capillary in a strong electric high-voltage field between the capillary electrode and the grounded electrode. The electric field distorts the drop on the tip of the capillary into a Taylor cone (formation of a single jet). The small liquid jet breaks down into numerous small charged primary droplets, drifting along field lines [31]. Electrospray (home-made) apparatus consists of the following: syringe bump (Kd Scientific) was used to keep the flow rate at 1 mL/h and power supply was 8 kV to generate the electric field. The distance between the nozzle and the collector was set to 7 cm. The deposition time was 7 min for each sample to get a thickness ~10 nm measured by AFM.

2.4. Characterization Techniques. The polymer nanocomposite films were analyzed with a Fourier transform infrared (FTIR) spectrophotometer Bruker Vertex 70 FTIR in the ATR mode. The UV-visible absorption spectra were recorded using V-630 UV/VIS spectrophotometer in the range of 1000–200 nm. The shape and particle size distribution of the nanoparticles were determined by using transmission

electron microscope JEOL-JEM-1011, Japan. Thin film thickness was measured using AFM-Thermo microscopes model (AutoProbe CP-Research Head).

2.5. Antimicrobial Activity. The antimicrobial activities of PAA/Ag nanocomposites deposited onto Si-wafer substrate by ESD technique were performed using disc diffusion agar technique against Gram negative bacteria *Escherichia coli* (*E. coli*), Gram positive bacteria *Bacillus subtilis* (*B. subtilis*), and fungi *Candida albicans* (*C. albicans*). Negative control of the prepared PAA films was tested under the same condition. After incubation at 37°C for 24 h for bacteria and 28°C for 48–72 h for fungi, the inhibition zones were recorded by measuring the average diameters of the clear zones.

3. Results and Discussion

3.1. UV-Visible Spectra

3.1.1. Effect of Ascorbic Acid (AA). The absorption spectra in ultraviolet and visible regions (UV-Vis) arise from electronic transitions in the molecules. Reduction of Ag^+ into Ag-NPs proceeds by electrons transfer from the reducing agent to the silver ions leading to the formation of silver atoms (Ag) and it was usually monitored by visual inspection and UV-Vis spectroscopy. Initially, the synthesis of Ag-NPs was confirmed by observing the color change of the reaction mixture. The appearance of a brown color suggested the formation of Ag-NPs [32]. Note that control experiments were performed in order to investigate the role of every chemical precursor on the synthetic process.

In the first step, the reaction medium contains PAA, $AgNO_3$, and $NaBH_4$ as a strong reducing agent. After 24 hours no remarkable color change was observed; that is, no Ag-NPs were formed. This observation was further confirmed by recording the UV-Vis absorption spectra as shown in Figure 1(a). The absorption spectrum did not show any absorption feature in the visible region. It was assumed that the PAA molecules reacted with silver salt solution forming a complex which is a more stable, so the reduction was rendered and/or inhibited.

In the second step, ascorbic acid (AA) as mild reducing agent was added to the mixture of PAA and $AgNO_3$. Thereafter, $NaBH_4$ was injected at once to the above mixture. A rapid change of the solution color from colorless to brown color was observed indicating an immediate reduction of the Ag^+ ions to Ag-NPs. The UV-Vis spectrum of this sample (Figure 1(b)) showed absorption peak at 425 nm which is attributed to the well-known surface plasmon resonance (SPR) of the Ag-NPs agreeing well with [33].

As the amount of AA increases in the polymeric solution, the band intensity increases; the maximum absorption wavelength is shifted towards lower UV region (hypsochromic shift) from 425 to 414 nm (Figure 1). The increase of the peaks intensity indicates that the concentration of Ag-NPs increases [34]. The symmetric and narrow absorption peaks imply the narrow size distribution of the silver nanoparticles at lower

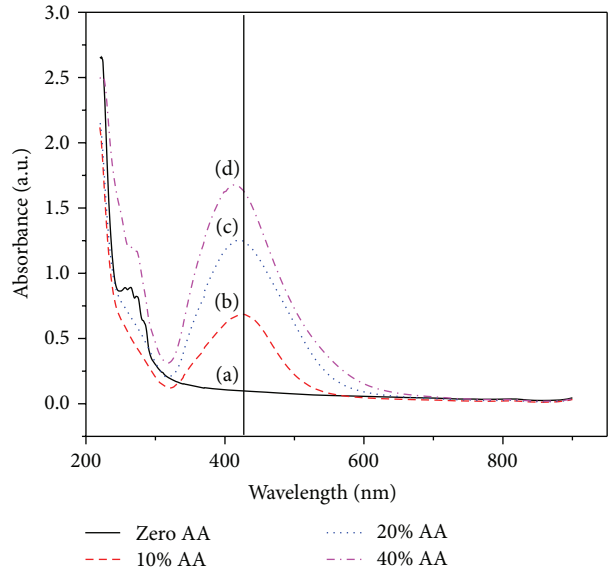

Figure 1: UV-Vis spectrum of PAA and $AgNO_3$ after addition of sodium tricitrate and $NaBH_4$ with different concentration of AA: 0 (a), 10 (b), 20 (c), and 40 (d) in μL.

AA loading. However, the blue shift of a maximum absorption wavelength implies that the size of silver nanoparticles decreases with increasing AA content and agreeing well with Xu et al.'s work [35].

For silver nanoparticles of λ_{max} values were reported in the visible range 400–500 nm [36]. The plasmon band of the Ag-NPs was noted at 425 nm corresponding to the formation of silver nanoparticles. It is likely that the role of AA is to catalyze the reduction reaction of Ag^+ ions from the solution to form nucleated particles. The addition of AA increases the reducing power of the reaction medium which in turn accelerates the rate of spontaneous nucleation. The more nucleating particles in the solution will result in raising the rate of agglomeration which can be seen by increasing the band width. However, the outlook of the prepared sample showed that the Ag-NPs were precipitated within 2 h. This was attributed to the continuous growth of the Ag-NPs leading to aggregation and/or agglomeration. Therefore, An-NPs are not stable and should be found a solution for that problem.

Tricitrate ion is a commonly used reducing agent in metal colloid synthesis; it undergoes strong surface interaction with silver nanocrystallites. The slow crystal growth was observed as a result of the interaction between the silver surface and the tricitrate ion makes this process unique compared to the other chemical and radiolytic synthetic methods [37].

3.1.2. Role of Sodium Tricitrate. In the final step of this synthetic pathway, sodium tricitrate was added to the mixture of (PAA + $AgNO_3$) before the addition of AA and $NaBH_4$. The change in color of the solution was observed in 30 min, that is, the addition of sodium tricitrate preventing immediate reduction of Ag^+ ions. Figure 2 shows the effect of sodium tricitrate with different volumes in the reaction mixture. Two more remarkable results were noted here.

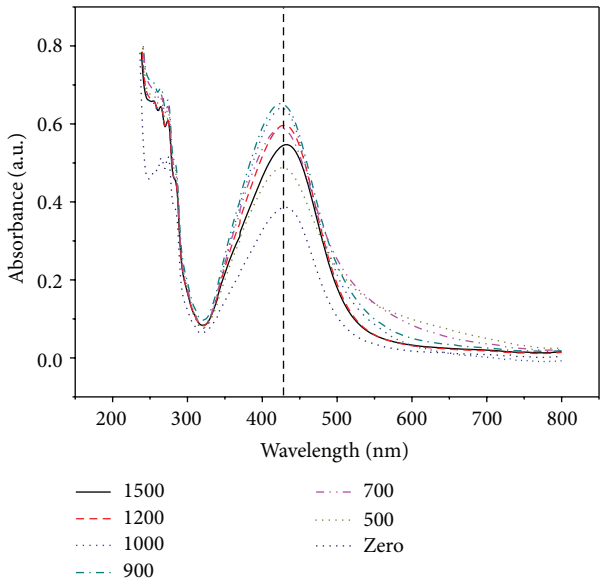

Figure 2: UV-Vis spectrum of PAA (0.1 mg) and $AgNO_3$ (0.5 mL) after addition of AA (10 μL) and $NaBH_4$ (10 μL) with different concentration of sodium citrate (in μL).

First, as the amount of sodium tricitrate increased (from 500 to 1000 μL), the plasmon band is shifted from 430 to 422 nm indicating quantum size effect that is formation of smaller particles. Presence of more stabilizing molecules in the medium inhibits the aggregation and/or the agglomeration of the Ag-NPs [38].

Second, the increased sodium tricitrate will increase the nucleation rate which results in formation of smaller particles. The plasmon peak gets narrower and sharper and also increases in the intensity with increasing sodium tricitrate. The symmetric and narrow absorption peak implies the narrow size distribution of the silver nanoparticles obtained by this method [39]. The presence of an equilibrium point observed with increasing tricitrate concentration confirms the existence of two species, complexed and uncomplexed silver nanoparticles. Such an interaction can be expressed in terms of equilibrium between PAA-Ag and tricitrate as the following:

$$\text{PAA-Ag} + \text{Citrate} \longleftrightarrow (\text{PAA-Ag-Citrate}) \quad (1)$$

Therefore, sodium tricitrate has unusual role of controlling the crystal growth and morphology of silver particles by capping the complex (PAA-Ag) so that it can protect Ag^+ from being instantly reduced.

3.1.3. Protecting Agent Effect. For preparing a homogeneous nanocomposite material containing Ag-NPs, one crucial issue is tendency for nanoparticles to aggregate, which leads to a loss of the peculiar properties associated with the nanoscale. For instance, in the area of antimicrobials, studies conducted by Lok et. al. [40] revealed that nonstabilized Ag-NPs prepared via standard chemical methods (the reduction of silver salt solutions) tend to aggregate in culture media and in biological buffers with a high salt content (chloride and phosphate are the most problematic anions).

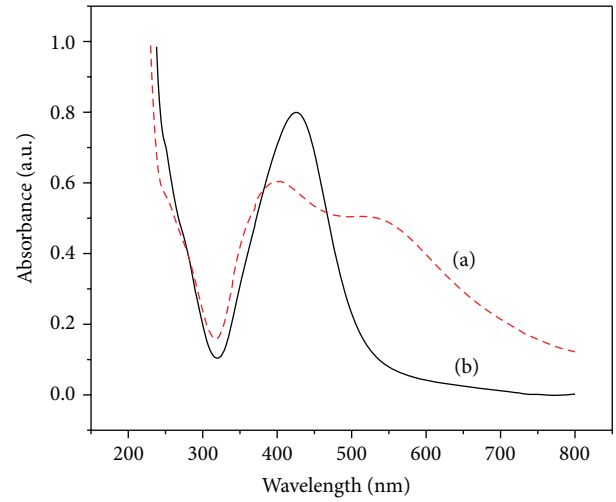

Figure 3: The UV-Vis spectrum of prepared Ag nanoparticles in absence of PAA (only: $AgNO_3$-AA-citrate-$NaBH_4$) (a) and in presence of PAA (PAA-$AgNO_3$-AA-citrate-$NaBH_4$) (b).

Generally, many organic molecules can bind to the particle surface and thus play the role of a stabilizer. The stabilization of metal nanoparticles was explained by the electronic interaction of the polymer functional groups with the metal particles. In fact, nucleophilic groups can bind the metal particles by donating electrons [41]. Protective reagents can coordinate metal ions before reduction, forming a complex that can then be reduced under mild conditions, these results in metal particles of smaller dimensions and a narrower size distribution than those obtained without protective polymers. Figure 3(a) shows the UV-Vis spectrum of prepared Ag nanoparticles in presence of $AgNO_3$-AA-citrate-$NaBH_4$ and absence of protective polymer (PAA) where Figure 3(b) shows the as-prepared PAA/Ag nanocomposite in presence of all additives together. Effect of these macromolecules can be attributed to the fact that either the particles are attached to the much larger protecting polymers, or the protecting molecules cover or encapsulate the metal particles, once the reduction process has occurred.

To study the protecting agent effect, different concentrations of PAA were applied (0.01, 0.1, 0.2, and 0.3 wt%). Figure 4 shows that, in presence of a low concentration of the polymer in the reaction medium, the intensity of plasmon peak was reduced.

It could be attributed to the smaller numbers of Ag nanoparticles or/and aggregation process were found. With increasing the concentration of PAA to 0.1 wt%, the intensity of plasmon peak was increased indicating the number of nucleation particles was raised and reaching equilibrium point between the amount of silver particles and polymer molecules in the reaction medium. In this case, with increasing the concentration of polymer, the intensity of the peak was reduced indicating that the protecting molecules covered or encapsulate the metal particles.

The stability of the Ag-NPs colloids were followed by detecting the alterations occurred on the surface plasmon peak of the Ag-NPs in our previous work [42]. It was found that the intensity of the absorption spectrum of PAA/Ag

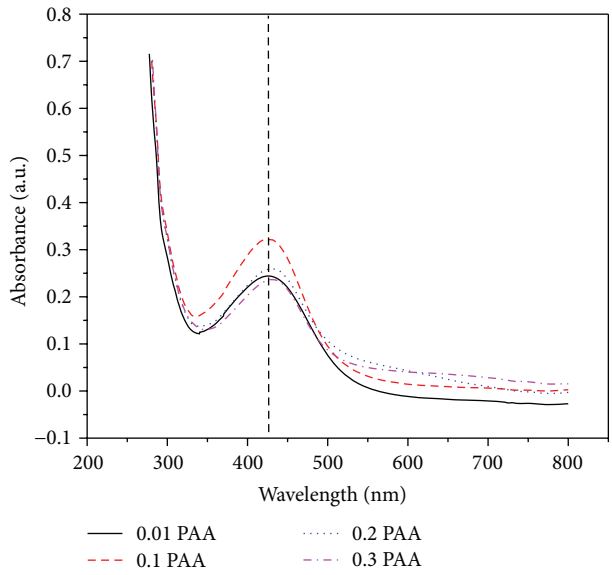

Figure 4: UV-Vis spectrum of as-prepared Ag-NPs in dependence on different concentrations of PAA.

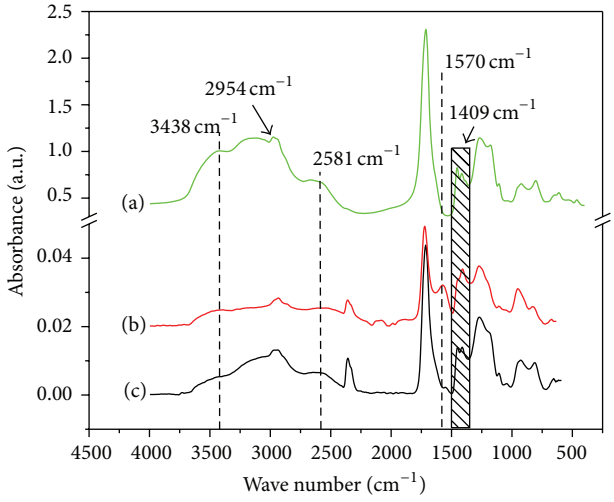

Figure 5: FTIR spectrum of (a) pure PAA, (b) PAA/Ag nanocomposites, and (c) PAA/$AgNO_3$.

nanocomposites was increased with a limit of aggregation process, indicating the stability of the prepared colloidal.

3.2. Chemical Composition. The FTIR spectra of PAA/$AgNO_3$ and PAA/Ag nanocomposite (PAA/$AgNO_3$/AA/citrate/$NaBH_4$) deposited by ESD in comparison to pure PAA in the region 4000–400 cm^{-1} were shown in Figure 5. One can see the typical characteristics of poly(acrylic acid) [43, 44]; that is, a wide band corresponding to stretching vibrations of hydroxyl group occurs in the range of 3700–3000 cm^{-1}. Negligible differences in the shape of this band before and after reacting of silver nitrate with PAA are result of –OH groups participating in hydrogen bands. Characteristic absorption bands appeared at 1651 cm^{-1} attributed to deformation vibrations of C–OH and two bands at 1559 cm^{-1} and 1324 cm^{-1} typical for carboxylate (symmetric stretching vibrations of carboxylate anion COO^-) occurred on the obtained FTIR spectra. The characteristic absorption band due to stretching vibration of C–O bond and deformation vibration of C–O–H appear at wave number 1246 cm^{-1} [45].

It is well known that poly(acrylic acid) shows typical intermolecular hydrogen bonds around 3170 cm^{-1} corresponding to bonded hydroxyl group (OH) and around 3400 cm^{-1} contribute the free hydroxyl group [46, 47]. The intensity of the band at ~3438 cm^{-1} was decreased in case of PAA/$AgNO_3$ mixture. This decrease can be referred to the intramolecular hydrogen bonding caused by the formation of novel interaction between the –CO(OH) groups in the PAA and silver nitrate particles (OH$\cdots$$AgNO_3$ bonding is formed). Consider that the carboxylic group shows normally a delocalized bonding of proton to oxygen atoms (COOH). Only in a specific reaction one can write –C(=O)OH. COOH groups of PAA react with Ag^0 to COO^- Ag^+ producing symmetric and asymmetric stretching vibrations.

Furthermore, the band at ~2581 cm^{-1}, in the pure PAA spectrum increased in the intensity and shifts significantly to the low frequency at 2527 cm^{-1} in the PAA/$AgNO_3$ and PAA/Ag nanocomposites spectrum. This change could be referred to the variation in the film thickness, because the pure PAA (blank) was investigated as powder with thickness ca. 1 μm, while the nanocomposites were characterized as ultra-thin film with thickness ca. 10 nm which was measured by AFM as mentioned in the characterization methods part and will be discussed later [48]; this is the first possibility. Another one is that it could be corresponded to the redeployment occurred and caused by the silver-acid interaction between the hydroxyl groups of PAA/Ag and the silver atom of unreacted $AgNO_3$ salt [42]. So that shift indicates a strong interaction occurred in this case (COO$\cdots$Ag). The FTIR analysis gives a great view on the changes occurred during the reaction and allowed defining different species of carbonyl groups in the PAA/Ag chains.

Carbonyl region, PAA, shows an intense band centered at 1713 cm^{-1} corresponding to stretching vibration of C=O group (Figure 5) [49, 50]. However, the appearance of a new band centered at 1570 cm^{-1} may be attributed to silver-acrylate asymmetric stretching or a complex formation between carboxylic groups and silver nanoparticles, corresponding to carbonyl Type III (Scheme 1) confirming that some amounts of free carbonyl groups remain as unreacted (Type I). In addition, the assignments of silver-acrylate asymmetric and symmetric bands are 1575 cm^{-1} = $\nu_{as}Ag^+C$ = O^- and 1409 cm^{-1} = ν_sAg^+C = O^-; the band situated at 1409 cm^{-1} was significantly increased in the intensity and might be assigned to the protons transfer from the –COOH groups to the nitrate groups (NO_3^-), which confirm the formation of ionic interactions between carboxylate and silver ions (Type IV).

3.3. Transmission Electron Microscopy (TEM). In order to determine the shape and size of the as-prepared Ag-NPs, the TEM micrographs were studied accordingly. Figure 6(a) showed the TEM micrographs of prepared silver nanoparticles in absence of PAA. The prepared clusters are

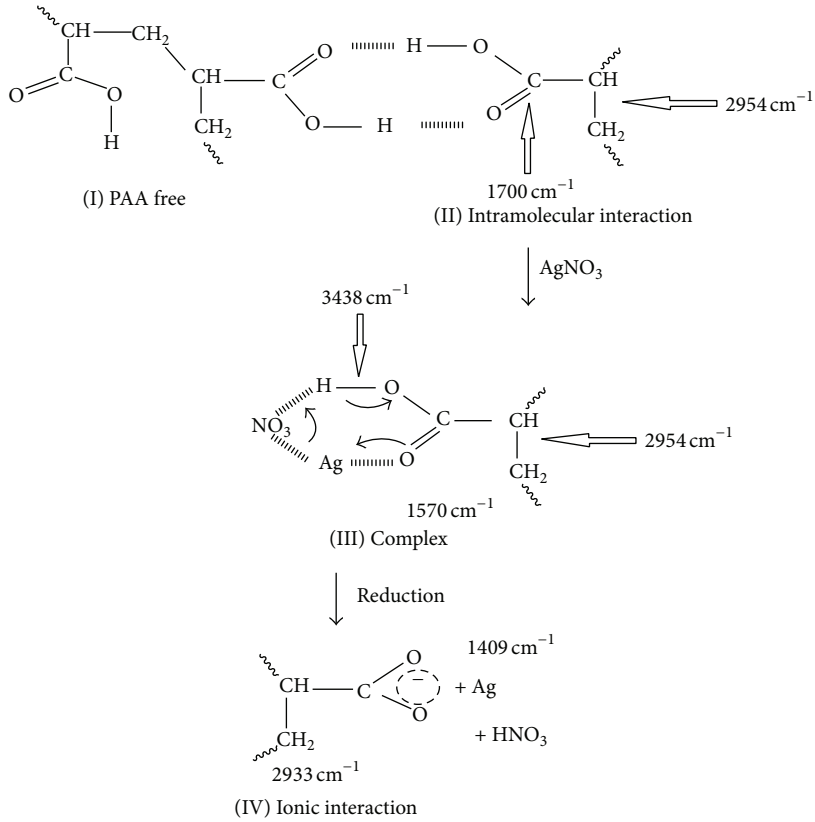

Scheme 1: Different types of association in the PAA/Ag nanocomposites as predicted by FTIR.

far away from monodispersion having a lot of aggregations which occurred. From the peak position of the Gaussian fitting, the average size of the Ag-NPs was determined equal to ~22 nm (Figure 6(c)). On the other hand, the Ag-NPs were prepared with a number of monodispersed spherical shapes and homogeneously distributed throughout the whole image field in presence of PAA (Figure 6(b)). In this case the average size of the Ag-NPs was equal to ~8 nm (Figure 6(d)). The formation of a uniform and well-shaped nanoparticle may be accounted as the result of using proper protecting and stabilizing agent which bind the surface of silver particles preventing the aggregation and stabilizing the nanoparticles in the solution.

3.4. Morphological Layers. In order to study the surface morphology of the prepared films atomic force microscope (AFM) was used. AFM has a great capability to investigate the roughness of the coated films over Si-wafer substrates.

Figure 7(a) presents the AFM images of the Si-wafer substrate as blank. The Si-wafer had an average roughness of 0.3 nm while pure PAA deposited on Si-wafer samples was 5.4 nm (Figure 7(b)). This means a homogenous and smooth surface with PAA deposited thin films by ESD method was obtained. However, Figure 7(b) shows that the surface of the substrate is not completely covered by a PAA film. The AFM images were recorded at different points on the surface which, in all cases, present the same morphology. It revealed a continuous and smooth surface covering the entire exposed area of the different samples, for all targets. Although several areas of the samples were scanned by AFM, only three images of the samples, one for each kind, were chosen for comparison. Moreover, Si-wafer was coated with PAA/Ag after reduction process with $NaBH_4$ in presence of AA and sodium tricitrate; the significant changes in the image of this sample can be seen (Figure 7(c)). There are still holes in the layer, so that there is no 100% coverage of the substrate which has taken place with roughness 43.6 nm. The nanoparticles play an important role to change the feature of films from smooth to rough one.

3.5. Antimicrobial Activities

3.5.1. Activity of Prepared Colloid. The activity of Ag-NPs embedded in polymeric matrix has a great effect for the prevention of growth and adherence of bacteria over the surface of some materials [51].

Recent studies indicated that the activity of Ag-NPs against bacteria mainly depends on the particle size [52]. Here the antimicrobial effects of PAA/Ag nanocomposites against pathogenic Gram negative, Gram positive bacteria, and fungi were investigated.

The prepared mixture without Ag-NPs was also tested as a control for comparison. 100 μL of samples was evaluated against pathogenic microorganisms and visualized after incubation at 37°C for 24 h for bacteria and 28°C for 48–72 h for fungi (Figure 8).

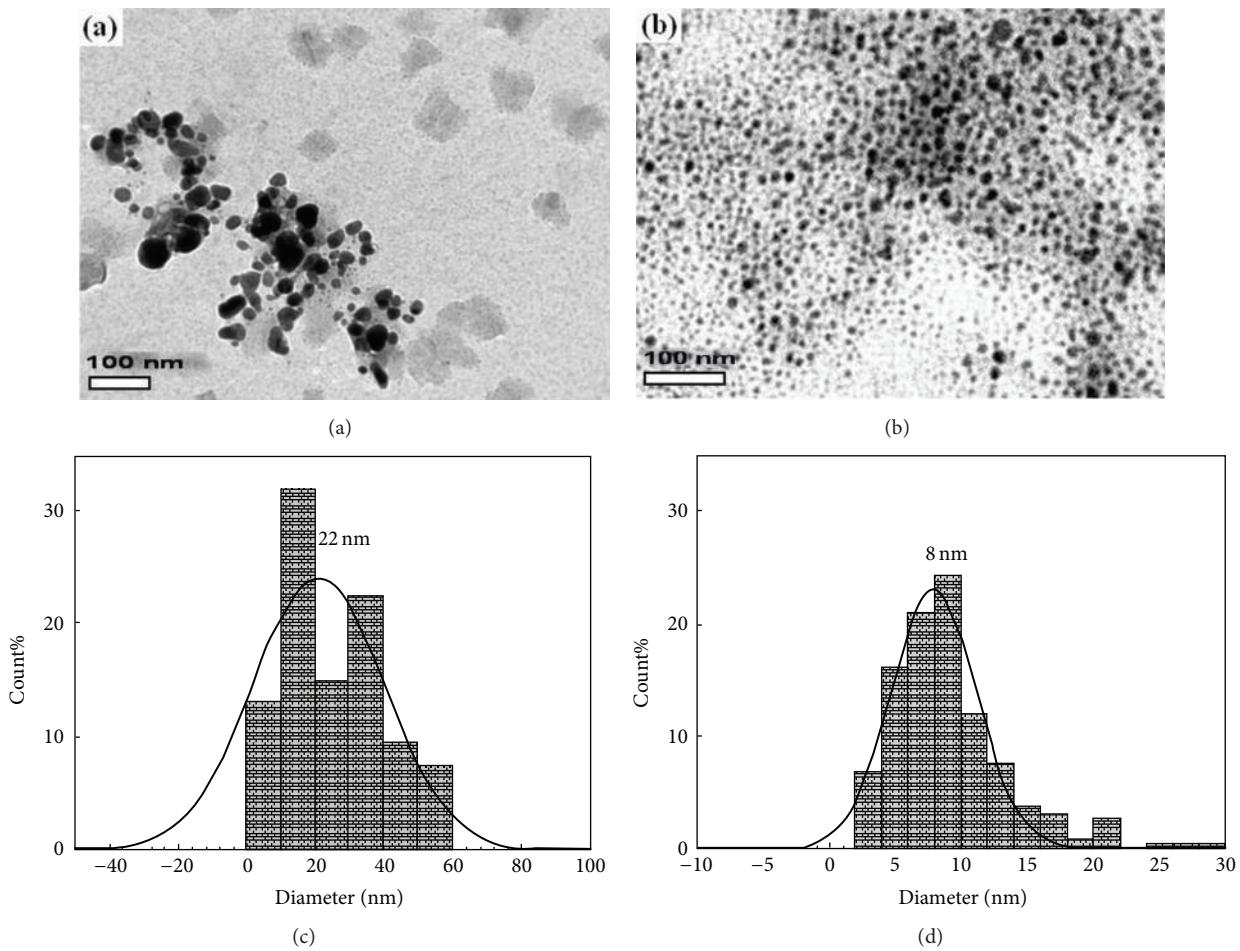

Figure 6: TEM micrographs of the as-prepared Ag-NPs (a) without and (b) with PAA and its corresponding histograms with Gaussian fitting (c) and (d), respectively.

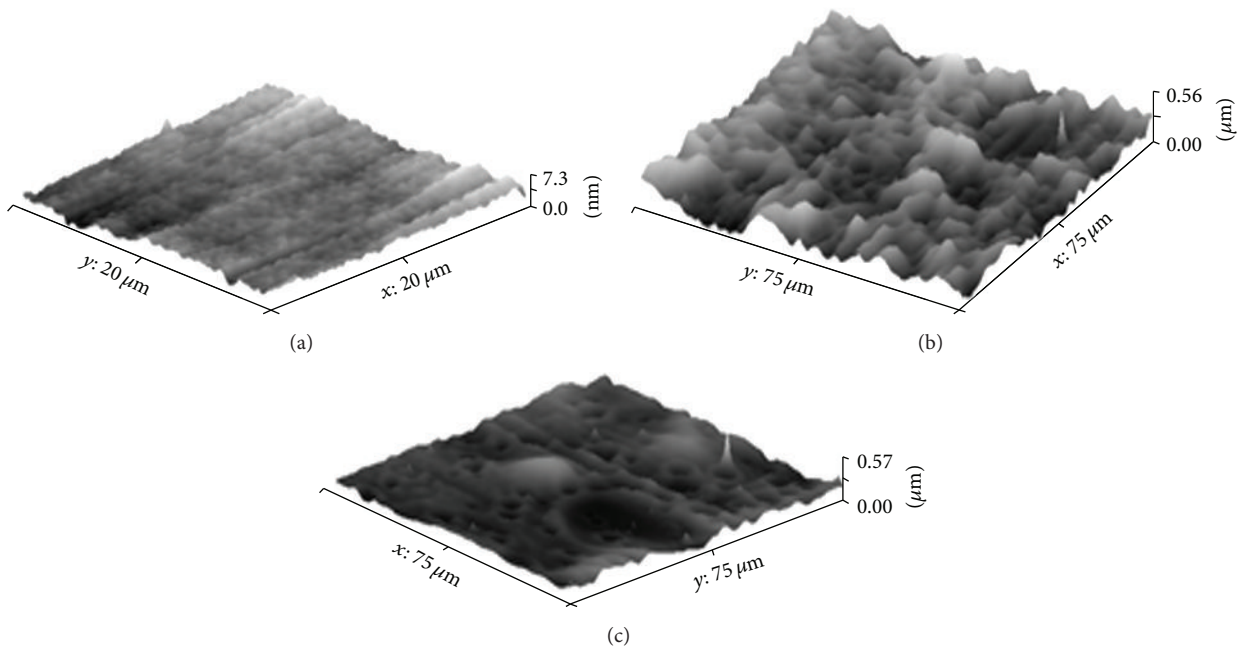

Figure 7: AFM-micrographs of (a) Si-wafer blank, (b) PAA coated Si-wafer, and (c) PAA/Ag after reduction spread on Si-wafer by means of ESD.

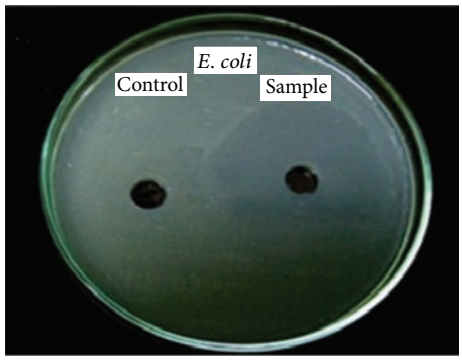

Figure 8: PAA/Ag nanocomposite inhibition zones against *E. coli* as example.

Table 1: Antimicrobial activity of prepared colloids by diffusion agar technique, well diameter: 6.0 mm of tested materials, inhibition zones measured in mm.

Tested microorganisms	Inhibition zones [mm]	Control
Gram positive bacteria		
B. subtilis	20.5 ± 0.58	NA
Gram negative bacteria		
E. coli	17.2 ± 0.25	NA
Fungi		
C. albicans	18.2 ± 0.58	NA

NA: no activity.

The control sample did not show any antimicrobial activity. On the other hand, a significant antibacterial property for PAA/Ag nanocomposites was observed due to the presence of Ag-NPs. Ag-NPs bind to the cell wall of the bacterial leading to bacteria death or cell distortion of the bacteria [53]. However, there was no activity observed for *P. aeruginosa* (Gram negative bacteria). Furthermore, the activity of prepared composite against microorganisms mainly depends on the rate of silver release and the amount of silver in the matrix. So under the preparation condition the results show that the synthesized nanocomposite has no activity against filamentous fungus *A. fumigatus*. According to the test results, the clear zone diameter for *S. aureus* and *Candida albicans* is 19.2 and 18.2 mm, respectively, which showed an important inhibition effect against Gram positive bacteria and fungi.

Table 1 listed the diameter measurements of inhibition zones which proved the ability of synthesized composite to inhibit the growth of selected bacteria and fungi. The results show that the efficacy was increased in the inhibition zone for Gram positive bacteria compared to Gram negative one and this may be attributed to the differences between cellular wall contents of Gram positive and Gram negative bacteria [54].

3.5.2. Activity of Deposited Films. Herein, the activity of prepared films of PAA/Ag nanocomposites deposited onto Si wafer substrate was tested. Control samples prepared by ESD films for pure PAA solution was investigated as a control for comparison. Otherwise, the significant antibacterial property for PAA/Ag nanocomposites films was observed due to the presence of Ag-NPs. The inhibition zones of tested microorganisms are significantly outlined. The clear zone can be related to the biological activity of the coated films containing PAA/Ag composite and it is measured based on the average diameter of inhibition zones in mm as shown in Table 2.

Table 2: Antimicrobial activity of prepared films by disc diffusion agar technique, inhibition zones measured in mm.

Tested microorganisms	PAA/Ag inhibition zones [mm]	Control
Gram positive bacteria		
B. subtilis	17	NA
Gram negative bacteria		
E. coli	16	NA
Fungi		
C. albicans	12	NA

Table 3: Optimum pH range for tested microorganisms.

Microorganisms	Optimum pH range
B. subtilis	4.0–8.0
E. coli	4.4–9.0
C. albicans	7.4 –8.0

Finally, according to the data obtained it could be established that Ag-NPs released from PAA/Ag nanocomposites matrix as colloidal or even as ultra-thin films are responsible for the antimicrobial effect. So it can be suggested that the prepared nanocomposites films with antibacterial properties could potentially be used as disinfecting surface coating, antimicrobial control systems, and water treatment systems.

3.5.3. Effect of pH Level. All microorganisms prefer a certain pH range. Changes of pH levels have the most noticeable effects on the growth of microorganisms and it means adding or subtracting hydrogen ions. Extreme changes of pH balance of the local environment tend to kill all microorganisms. Bacteria were classified into three types according to the pH level (1) an acidophile, (2) neutrophil, and (3) alkaliphile. An acidophile grows in a pH range of 1 to 5.9, a neutrophil between 6.0 and 9.0, and an alkaliphile between 9 and 11. Most grow in a range between 4.0 and 9.0 (neutrophils). For example, Table 3 listed some optimum pH range for tested microorganisms [55–57].

Knowing the effects of pH level on bacteria is essential for those working in the food inspection sector. Although raising the pH level of bacteria may kill them, this does not necessarily result in preventing bacteria from growing in any particular environment. Changing the pH level to eliminate one species of bacteria may give rise to another species that can live in the new pH level [58].

Table 4 shows the pH values for all steps during the synthetic pathway for the preparation of PAA/Ag nanocomposites.

Table 4: pH results during all steps in the synthetic pathway.

Reaction steps	pH
Step 1 (PAA/$AgNO_3$/$NaBH_4$)	3.6
Step 2 (PAA/$AgNO_3$/AA/$NaBH_4$)	2.6
Step 3 (PAA/$AgNO_3$/tricitrate/AA/$NaBH_4$)	6.3

As shown in Table 4, pH value of PAA/Ag nanocomposite was 6.3 in the same optimum range for the growth of tested strains (Table 3). So, it can be concluded that the antimicrobial activity results were due to the presence of Ag-NPs.

4. Conclusion

Thin PAA/Ag nanocomposite films were successfully prepared using electrospray deposition techniques with highly dispersed Ag-NPs in comparison to traditional casting one. A strong reducing mixture of $NaBH_4$ and ascorbic acid were used to release Ag-NPs in the polymer matrix. In presence of sodium tricitrate the stability of nanoparticles was improved. The citrate hinders agglomeration of the syntheses particles. The Ag-NPs in the polymeric matrix and in existence of AA and citrate distributed well with an average particle size of around 8 nm as revealed by TEM image. The formation of uniform and well-shaped nanoparticles was accounted as a result of using proper surfactant (sodium tricitrate) and protecting agent (PAA). The antibacterial activity towards different kinds of bacteria and fungi was investigated. Results indicated that PAA/Ag have antimicrobial action against Gram negative, Gram positive bacteria, and fungi. Therefore, the prepared nanocomposite films with antibacterial properties could potentially be used as disinfecting surface coating and antimicrobial control systems.

Additional Points

In the next work, we are going to study the durability of this thin film coating such as mechanical properties, thermal stability, and adhesion.

Competing Interests

The authors declare that there are no competing interests regarding the publication of this paper.

References

[1] W. E. Stamm, "Infections related to medical devices," *Annals of Internal Medicine*, vol. 89, no. 5, pp. 764–769, 1978.

[2] A. E. Madkour and G. N. Tew, "Towards self-sterilizing medical devices: controlling infection," *Polymer International*, vol. 57, no. 1, pp. 6–10, 2008.

[3] J. S. Kim, E. Kuk, K. N. Yu et al., "Antimicrobial effects of silver nanoparticles," *Nanomedicine: Nanotechnology, Biology, and Medicine*, vol. 3, no. 1, pp. 95–101, 2007.

[4] N. L. Lala, R. Ramaseshan, L. Bojun et al., "Fabrication of nanofibers with antimicrobial functionality used as filters: protection against bacterial contaminants," *Biotechnology and Bioengineering*, vol. 97, no. 6, pp. 1357–1365, 2007.

[5] H. Butt, K. Graf, and M. Kappl, "Front matter," in *Physics and Chemistry of Interfaces*, pp. 206–219, Wiley VCH, New York, NY, USA, 2003.

[6] B. Ahmmad, J. Kurawaki, K. Leonard, and Y. Kusumoto, "Biosynthesis of silver and gold nanoparticles: effect of microwave irradiation," *Journal of Scientific Research*, vol. 2, no. 3, pp. 495–500, 2010.

[7] M.-C. Daniel and D. Astruc, "Gold nanoparticles: assembly, supramolecular chemistry, quantum-size-related properties, and applications toward biology, catalysis, and nanotechnology," *Chemical Reviews*, vol. 104, no. 1, pp. 293–346, 2004.

[8] S. Ghosh, U. Anand, and S. Mukherjee, "Investigating the evolution of drug mediated silver nanoparticles," *Analyst*, vol. 138, no. 15, pp. 4270–4274, 2013.

[9] T. E. Abbott Chalew, G. S. Ajmani, H. Huang, and K. J. Schwab, "Evaluating nanoparticle breakthrough during drinking water treatment," *Environmental Health Perspectives*, vol. 121, no. 10, pp. 1161–1166, 2013.

[10] J. Baharara, F. Namvar, T. Ramezani, N. Hosseini, and R. Mohamad, "Green synthesis of silver nanoparticles using *Achillea biebersteinii* flower extract and its anti-angiogenic properties in the rat aortic ring model," *Molecules*, vol. 19, no. 4, pp. 4624–4634, 2014.

[11] A. Gautam and F. C. J. M. Van Veggel, "Synthesis of nanoparticles, their biocompatibility, and toxicity behavior for biomedical applications," *Journal of Materials Chemistry B*, vol. 1, no. 39, pp. 5186–5200, 2013.

[12] P. V. AshaRani, G. L. K. Mun, M. P. Hande, and S. Valiyaveettil, "Cytotoxicity and genotoxicity of silver nanoparticles in human cells," *ACS Nano*, vol. 3, no. 2, pp. 279–290, 2009.

[13] J. R. Morones, J. L. Elechiguerra, A. Camacho et al., "The bactericidal effect of silver nanoparticles," *Nanotechnology*, vol. 16, no. 10, pp. 2346–2353, 2005.

[14] S. He, J. Yao, P. Jiang et al., "Formation of silver nanoparticles and self-assembled two-dimensional ordered superlattice," *Langmuir*, vol. 17, no. 5, pp. 1571–1575, 2001.

[15] M. Maillard, P. Huang, and L. Brus, "Silver nanodisk growth by surface plasmon enhanced photoreduction of adsorbed [Ag^+]," *Nano Letters*, vol. 3, no. 11, pp. 1611–1615, 2003.

[16] E. Hao, K. L. Kelly, J. T. Hupp, and G. C. Schatz, "Synthesis of silver nanodisks using polystyrene mesospheres as templates," *Journal of the American Chemical Society*, vol. 124, no. 51, pp. 15182–15183, 2002.

[17] J. B. Jackson and N. J. Halas, "Silver nanoshells: variations in morphologies and optical properties," *The Journal of Physical Chemistry B*, vol. 105, no. 14, pp. 2743–2746, 2001.

[18] M. P. Mallin and C. J. Murphy, "Solution-phase synthesis of sub-10 nm Au-Ag alloy nanoparticles," *Nano Letters*, vol. 2, no. 11, pp. 1235–1237, 2002.

[19] A. Fahmy, A. Al-Zomarawy, A. Z. Sayed, M. A. Ezz El-Arab, H. A. Shehata, and A. M. Saeed, "Silver/polyethylene glycol nanocomposite thin films and its biological applications," *Journal of Advances in Chemistry*, vol. 11, no. 5, pp. 3597–3608, 2015.

[20] A. Henglein, "Preparation and optical aborption spectra of $Au_{core}Pt_{shell}$ and $Pt_{core}Au_{shell}$ colloidal nanoparticles in aqueous solution," *The Journal of Physical Chemistry B*, vol. 104, no. 10, pp. 2201–2203, 2000.

[21] H. Sakai, T. Kanda, H. Shibata, T. Ohkubo, and M. Abe, "Preparation of highly dispersed core/shell-type titania nanocapsules

containing a single Ag nanoparticle," *Journal of the American Chemical Society*, vol. 128, no. 15, pp. 4944–4945, 2006.

[22] C. C. Chusuei, X. Lai, K. Luo, and D. W. Goodman, "Modeling heterogeneous catalysts: metal clusters on planar oxide supports," *Topics in Catalysis*, vol. 14, no. 1–4, pp. 71–83, 2000.

[23] I. Pastoriza-Santos and L. M. Liz-Marzán, "Formation of PVP-protected metal nanoparticles in DMF," *Langmuir*, vol. 18, no. 7, pp. 2888–2894, 2002.

[24] P. Raveendran, J. Fu, and S. L. Wallen, "Completely 'green' synthesis and stabilization of metal nanoparticles," *Journal of the American Chemical Society*, vol. 125, no. 46, pp. 13940–13941, 2003.

[25] N. R. Jana, L. Gearheart, and C. J. Murphy, "Seed-mediated growth approach for shape-controlled synthesis of spheroidal and rod-like gold nanoparticles using a surfactant template," *Chemistry of Materials*, vol. 13, pp. 1389–1393, 2001.

[26] H. Huang and X. Yang, "Synthesis of polysaccharide-stabilized gold and silver nanoparticles: a green method," *Carbohydrate Research*, vol. 339, no. 15, pp. 2627–2631, 2004.

[27] T. Kim, S. Nam, S. Lim, and H. Kim, "Facile in-situ preparation of poly(acrylic acid)-silver nanocomposite thin films with highly dispersed silver nanoparticles," *Molecular Crystals and Liquid Crystals*, vol. 568, no. 1, pp. 170–178, 2012.

[28] N. Haddadine-Rahmoun, F. Amrani, V. Arrighi, and J. M. G. Cowie, "Interpolymer complexation in hydrolysed poly(styrene-co-maleic anhydride)/poly(styrene-co-4-vinylpyridine)," *European Polymer Journal*, vol. 44, no. 3, pp. 821–831, 2008.

[29] N. Bouslah, N. Haddadine, F. Amrani, and R. Hammachin, "Comparison of specific interactions in P4VP/PSCA and PS4VP/PSCA blends and complexes," *Journal of Applied Polymer Science*, vol. 108, no. 5, pp. 3256–3261, 2008.

[30] J. H. Kim, J. Won, and Y. S. Kang, "Preparation of poly(ethylene glycol) brushes on polysulfone membranes for olefin/paraffin separation," *Langmuir*, vol. 16, no. 24, pp. 9662–9665, 2000.

[31] K. Altmann, R.-D. Schulze, and J. Friedrich, "Polymer deposition morphology by electrospray deposition—modifications through distance variation," *Thin Solid Films*, vol. 564, pp. 269–276, 2014.

[32] J. Y. Song and B. S. Kim, "Rapid biological synthesis of silver nanoparticles using plant leaf extracts," *Bioprocess and Biosystems Engineering*, vol. 32, no. 1, pp. 79–84, 2009.

[33] M. F. Zayed, W. H. Eisa, and A. A. Shabaka, "Malva parviflora extract assisted green synthesis of silver nanoparticles," *Spectrochimica Acta Part A: Molecular and Biomolecular Spectroscopy*, vol. 98, pp. 423–428, 2012.

[34] W. Z. Zhang, X. L. Qiao, and J. G. Chen, "Synthesis and characterization of silver nanoparticles in AOT microemulsion system," *Chemical Physics*, vol. 330, no. 3, pp. 495–500, 2006.

[35] G.-N. Xu, X.-L. Qiao, X.-L. Qiu, and J.-G. Chen, "Preparation and characterization of stable monodisperse silver nanoparticles via photoreduction," *Colloids and Surfaces A: Physicochemical and Engineering Aspects*, vol. 320, no. 1–3, pp. 222–226, 2008.

[36] N. Mohri, M. lnoue, Y. Arai, and K. Yoshikawa, "Kinetic study on monolayr formation with 4-aminobenzenethiol on a gold surface," *Langmuir*, vol. 11, pp. 1612–1616, 1995.

[37] Z. S. Pillai and P. V. Kamat, "What factors control the size and shape of silver nanoparticles in the citrate ion reduction method?" *Journal of Physical Chemistry B*, vol. 108, no. 3, pp. 945–951, 2004.

[38] Y. Liu, S. Chen, L. Zhong, and G. Wu, "Preparation of high-stable silver nanoparticle dispersion by using sodium alginate as a stabilizer under gamma radiation," *Radiation Physics and Chemistry*, vol. 78, no. 4, pp. 251–255, 2009.

[39] G. Suyal, "Bimetallic colloids of silver and copper in thin films: sol–gel synthesis and characterization," *Thin Solid Films*, vol. 426, no. 1-2, pp. 53–61, 2003.

[40] C.-N. Lok, C.-M. Ho, R. Chen et al., "Proteomic analysis of the mode of antibacterial action of silver nanoparticles," *Journal of Proteome Research*, vol. 5, no. 4, pp. 916–924, 2006.

[41] C. S. R. Kumar, *Nanocomposites*, John Wiley & Sons, 2010.

[42] A. Fahmy, W. H. Eisa, M. Yosef, A. Hassan, and H. Hammad, "Electrosprayed of polyacrylic acid/silver nanocomposite thin films and its antimicrobial application," *Middle East Journal of Applied Sciences*, vol. 5, no. 2, pp. 395–403, 2015.

[43] O. Carton, D. Ben Salem, S. Bhatt, J. Pulpytel, and F. Arefi-Khonsari, "Plasma polymerization of acrylic acid by atmospheric pressure nitrogen plasma jet for biomedical applications," *Plasma Processes and Polymers*, vol. 9, no. 10, pp. 984–993, 2012.

[44] A. Fahmy, R. Mix, A. Schönhals, and J. F. Friedrich, "Structure of plasma-deposited poly(acrylic acid) films," *Plasma Processes and Polymers*, vol. 8, no. 2, pp. 147–159, 2011.

[45] B. Grabowska and M. Holtzer, "Structural examination of the cross-linking reaction mechanism of polyacrylate binding agents," *Archives of Metallurgy and Materials*, vol. 54, no. 2, pp. 427–437, 2009.

[46] A. Fahmy, T. A. Mohamed, and A. Schönhals, "Structure of plasma poly(acrylic acid): influence of pressure and dielectric properties," *Plasma Chemistry and Plasma Processing*, vol. 35, no. 2, pp. 303–320, 2015.

[47] J. Dong, Y. Ozaki, and K. Nakashima, "Infrared, Raman, and near-infrared spectroscopic evidence for the coexistence of various hydrogen-bond forms in poly(acrylic acid)," *Macromolecules*, vol. 30, no. 4, pp. 1111–1117, 1997.

[48] G. L. Powell, M. Milosevic, J. Lucania, and N. J. Harrick, "The Spectropus™ system: remote sampling accessories for reflectance, emission, and transmission analysis using Fourier transform infrared spectroscopy," *Applied Spectroscopy*, vol. 46, pp. 111–125, 1992.

[49] A. Fahmy, R. Mix, A. Schönhals, and J. Friedrich, "Structure of plasma-deposited copolymer films prepared from acrylic acid and styrene: part II variation of the comonomer ratio," *Plasma Processes and Polymers*, vol. 10, no. 9, pp. 750–760, 2013.

[50] A. Fahmy, D. Debarnot, and J. Friedrich, "Influence of water on the structure of plasma deposited allyl alcohol polymer layers," *Journal of Adhesion Science and Technology*, vol. 29, no. 10, pp. 965–980, 2015.

[51] H. V. Tran, L. D. Tran, C. T. Ba, H. D. Vu, T. N. Nguyen, and D. G. Pham, "Synthesis, characterization, antibacterial and antiproliferative activities of monodisperse chitosan-based silver nanoparticles," *Colloids and Surfaces A Physicochemical and Engineering Aspects*, vol. 360, no. 1–3, pp. 32–40, 2010.

[52] S. Chalal, N. Haddadine, N. Bouslah, and A. Benaboura, "Preparation of poly(acrylic acid)/silver nanocomposite by simultaneous polymerization-reduction approach for antimicrobial application," *Journal of Polymer Research*, vol. 19, no. 12, pp. 24–31, 2012.

[53] J. J. Castellano, S. M. Shafii, F. Ko et al., "Comparative evaluation of silver-containing antimicrobial dressings and drugs," *International Wound Journal*, vol. 4, no. 2, pp. 114–140, 2007.

[54] A. Celebioglu, Z. Aytac, O. C. O. Umu, A. Dana, T. Tekinay, and T. Uyar, "One-step synthesis of size-tunable Ag nanoparticles incorporated in electrospun PVA/cyclodextrin nanofibers," *Carbohydrate Polymers*, vol. 99, pp. 808–816, 2014.

[55] M. J. Tevethia and M. Mandel, "Effects of pH on transformation of Bacillus subtilis with single-stranded deoxyribonucleic acid," *Journal of Bacteriology*, vol. 106, no. 3, pp. 802–807, 1971.

[56] K. A. Presser, D. A. Ratkowsky, and T. Ross, "Modelling the growth rate of *Escherichia coli* as a function of pH and lactic acid concentration," *Applied and Environmental Microbiology*, vol. 63, no. 6, pp. 2355–2360, 1997.

[57] S. Nadeem, A. Shafiq, S. Hakim, Y. Anjum, and S. U. Kazm, "Effect of growth media, pH and temperature on yeast to hyphal transition in Candida albicans," *Journal of Medical Microbiology*, vol. 3, pp. 185–192, 2013.

[58] R. Huebsch, http://www.ehow.com/about_5695904_effects-pH-bacterial-growth.html.